Correlation of real-time MRTI and post-treatment MRI with histologic depiction of prostatic ablation using high-intensity ultrasound

G. Sommer[1], K. Butts[1], D. Bouley[2], B. Daniel[1], T. Ross[3], W. Nau[3], C. Diederich[3]

[1]Dept. of Radiology, Stanford University, Stanford, CA, United States, [2]Dept. of Comparative Medicine, Stanford University, Stanford, CA, United States, [3]UCSF Radiation Oncology, San Francisco, CA, United States

Introduction:

Prostatic tissue may be ablated using high-intensity ultrasonic applicators either directly inserted into the prostate gland (interstitial applicators) or inserted through the urethra (1) (transurethral applicators). Using magnetic resonance temperature imaging (MRTI) based on proton resonance frequency, it is possible to monitor the deliver of ultrasonic heating in real-time (2), and MRI may also be useful in depicting the spatial distribution of ablated and viable prostatic tissue following the delivery of heating to the prostate. Studies were performed to assess the degree of heating, as depicted with MRTI required to ablate prostate tissue *in vivo*, and determine the ability of MR imaging to accurately depict ablated prostate tissue.

Methods:

In vivo studies of high-intensity ultrasonic ablation of prostate tissue were performed for 7 dogs in a 0.5 T system (Signa-SP, General Electric Corp.). Prostate tissue was ablated under real-time guidance using MRTI in 3 simultaneous axial planes, based on PRF techniques. Either interstitial or transurethral applicators, which were MRI compatible, were employed to ablate selected regions of the prostate gland in each study. The transurethral applicators varied in their degrees of ultrasonic directivity or focussing. Following the ablative procedures, T2-weighted FSE, line-scanned DWI, and post-gadolinium T1-weighted imaging of the prostate was performed. Cumulative maximum temperature and T_{43} equivalent maps of the prostate were also calculated. All dogs were sacrificed at the end of the procedure, and prostates were removed, sectioned at 5 mm. Intervals, and stained with the vital stain TTC and standard hematoxylin and eosin (H and E). The temperature maps created from the studies, and post-ablation MR images were correlated with the histologic distributions of ablation present in the prostates, and the ablated prostates were examined microscopically

Results:

Correlation of cumulative maximum temperature maps and T_{43} equivalent maps with histologic sections at corresponding levels in the prostate gland indicated a good correlation between cumulative T_{max} of ~52 °C and t_{43}> 240 min with viable tissue boundaries as visualized in TTC-stained sections. Similar correlations between the post-ablation T2-weighted, DWI and post-contrast T1-weighted images and corresponding histologic sections indicated that the acutely ablated regions were not discernible in T2-weighted images, but were detectable as regions of reduced ADC in DW images. Post-contrast T1-weighted images demonstrated the ablated regions with high SNR, as zones of diminished perfusion, often with an enhancing rim. Further histologic and microscopic study indicated that the ablated regions generally consisted of a "perimeter zone" revealing obvious tissue damage characterized by fragmentation and necrosis. A larger "heat fixed" region of necrosis was typically present centrally, showing very subtle changes from normal prostate, compared to the perimeter zone damage. Correlative temperature data from real-time MRTI, post treatment MR images and histologic results from the same case of prostate ablation, in which 2 regions of a canine prostate were ablated using a 90° cylindrical transurethral applicator in 2 separate 10-minute heating sequences are shown in Figures 1 and 2 below.

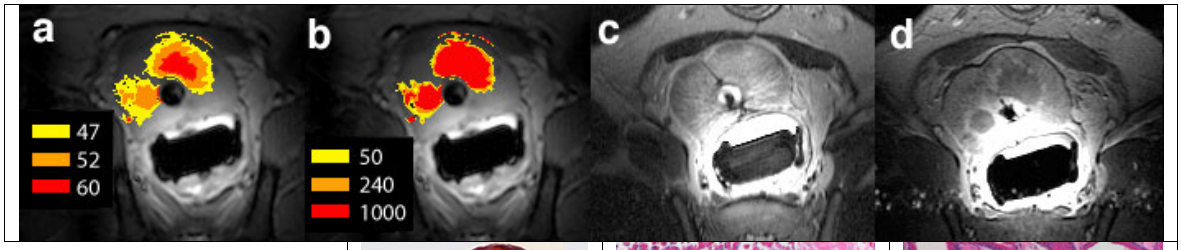

Figure 1: (right) (a) Cumulative temperature map (°C) and (b) t_{43} equivalent map with correlative T2-weighted (c) and post-contrast T1-weighted (d) MR images following ablation.

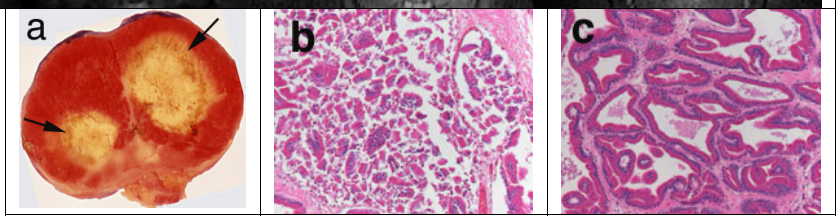

Figure 2: (right) (a) TTC-stained histologic section of ablated canine prostate at the level demonstrated in the MR images of Figure 1. Viable tissue is stained red-orange, and the ablated regions are pale, with the "perimeter zone" of ablation indicated with arrows. Low-power magnification (H+E) of the prostate shows (b) marked tissue destruction in the perimeter zone and (c) relatively normal-appearing "heat-fixed" prostate centrally.

Discussion:

Using MRTI, it was possible to monitor prostatic heating and ablation created with high-intensity ultrasonic applicators, with the zones of ablation corresponding well to cumulative temperature maps indicating T_{max} of ~52 °C and t_{43}> 240 min. In this acute model of prostatic ablation, T2-weighted imaging did not reveal ablated regions of prostate, but ablated regions were identifiable as zones of reduced ADC in DW images. Post-contrast T1-weighted images gave the best depiction of the ablated regions, with the large region of "heat-fixed" prostate showing reduced perfusion compared to normal prostate, and the "perimeter zone" of ablation suggested by a rim of increased enhancement. Similar ablative patterns have been reported by Coad et al. in liver tissue (3).

References:

1. Hazle JD, Diederich CJ, Kangasniemi M, Price RE, Olsson LE, Stafford RJ. MRI-guided thermal therapy of transplanted tumors in the canine prostate using a directional transurethral ultrasound applicator. J Magn Reson Imaging. 2002 Apr;15(4):409-17.

2. Peters RD, Chan E, Trachtenberg J, Jothy S, Kapusta L, Kucharczyk W, Henkelman RM. Magnetic resonance thermometry for predicting thermal damage: an application of interstitial laser coagulation in an in vivo canine prostate model. Magn Reson Med. 2000 Dec;44(6):873-83.

3. Coad JE, Kosari K, Humar A, Sielaff TD. "Radiofrequency ablation causes thermal fixation of hepatocellular carcinoma". Clin Transplant. 2003

Acknowledgement:

This work was partially supported by grants CA 79931, CA88205 and DK51939 from the NIH.